Nanoparticle Metal−Semiconductor Charge Transfer in ZnO/PATP/Ag Assemblies by Surface-Enhanced Raman Spectroscopy

Zhihua Sun,[†] Chunxu Wang,[†] Jingxiu Yang,[†] Bing Zhao,*[,†] and John R. Lombardi*[,‡]

State Key Laboratory of Supramolecular Structure and Materials, Jilin University, 2699 Qianjin Avenue, Changchun, 130012, People's Republic of China, and Department of Chemistry, The City College of New York, New York, New York 10031

Received: November 27, 2007; In Final Form: January 11, 2008

The ZnO/PATP/Ag sandwich structure and its reverse Ag/PATP/ZnO were fabricated using ZnO nanorods and silver nanoparticles with functional molecules 4-aminothiophenol (PATP) through layer-by-layer self-assembly techniques. Under near-IR excitation (1064 nm, far from the surface plasmon resonance of the Ag nanoparticles in the assemblies), the enhancement of surface-enhanced Raman spectra (SERS) from the charge-transfer mechanism can be readily observed only in the former structure. The considerably larger enhancement of the b_2 modes, relative to those of the a_1 modes, is ascribed to the charge transfer between the silver nanoparticles and ZnO tunneling through the interconnecting PATP molecules. This is not observed in the second structure. The result demonstrates for the first time that directional charge transfer between nanoscale metal and semiconductor tunneling through the interconnecting molecules may be examined by SERS.

I. Introduction

Surface-enhanced Raman spectroscopy (SERS) has become a widely used tool for the investigation of properties of various nanoscale structures. The high sensitivity and resolution of the technique make it ideal for extracting detailed information as to the nature of molecular interactions with both metal and semiconductor particles.[1−6] SERS is characterized by both surface plasmon resonance as well as charge-transfer effects.[7−14] The surface plasmon resonance comes about due to the interaction of the exciting laser frequency with the metal conduction band electrons, and at certain particle sizes very large electric fields are produced at the nanoparticle surface. When these fields interact with an adsorbed molecule, enormous enhancements are observed in the molecular Raman signal. Additional contributions to the observed enhancements have been attributed to charge-transfer transitions induced by the molecule−metal interaction.[13] At certain excitation wavelengths, electrons can be transferred between the molecule either to or from the metal conduction band, adding additional intensity to the enhanced Raman signal. However, the charge-transfer mechanism has a strong effect on the observed Raman spectrum. Although the vibrational frequencies of the molecule are not strongly affected by SERS, their relative intensities are. As a result charge transfer is often accompanied by drastic changes in the observed SERS spectrum.

SERS has also recently been observed in semiconductor nanoparticles.[15−19] Since these particles often have plasmon resonances far from the excitation wavelengths used, it is widely assumed that the charge-transfer mechanism dominates these spectra. This line of research holds great promise in that it is increasingly possible to produce samples of well-controlled nanoparticle sizes and shapes.

It is also possible to combine both metals and semiconductors into composite systems, with interesting properties. The interface between metals and semiconductors is often called a "Schottky barrier", and these have been widely investigated in bulk systems.[20,21] An important feature of such systems is the appearance of a dipolar layer at the junction, which mediates the energies of the interconnecting systems. More recently a ZnO core−Ag shell quantum dot system was studied by Shan et al.[22] They used SERS to observe enhancements in the LO phonon modes of the ZnO core, observing up to five overtones. They attributed the observations to charge transfer from the silver conduction band into the ZnO core, red-shifting the plasmon resonance and greatly enhancing the (normally weak) phonon spectrum.

In another study, Zhou et al.[23] investigated charge transfer between adjacent Ag nanoparticles mediated by a connecting molecule *p*-aminothiophenol (PATP). The thiol (−SH) end of the molecule forms a strong bond to the first silver nanoparticle, and a subsequent addition of additional Ag nanoparticles can then bind to the remaining amino group, forming a sandwich-like structure connecting two Ag particles. The resultant SERS spectrum showed very strong enhancement of the nontotally symmetric b_2 vibrational modes relative to the a_1 modes. This has been shown to be characteristic of charge transfer in a metal−PATP system[24] by a density functional theory (DFT) calculation with PATP on Au nanoparticles. In a further study[25,26] in which PATP was sandwiched between Au and Ag nanoparticles (Au/PATP/Ag; taking advantage of the differential adsorption of the thiol and amino ends of the molecule), the authors were able to effect charge transfer between two different types of particles (i.e., Ag → Au) with different work functions (4.3 eV for Ag and 5.0 eV for Au). The mechanism was attributed to tunneling through the intermediate PATP molecule. Once again the enhancement of the b_2 modes of the PATP was considered important in the conversion. The charge transfer was aided by the quinoid dipolar resonance structure forming a net positive charge on the $-NH_2$ and negative charge on the −SH

* Corresponding authors. Fax: +86-431-85193421 (B.Z.). E-mail: zhaob@mail.jlu.edu.cn (B.Z.), lombardi@sci.ccny.cuny.edu (J.R.L.).
† Jilin University.
‡ The City College of New York.

10.1021/jp711240a CCC: $40.75
Published on Web 03/25/2008

ends of the molecule. When the sandwich was reversed (i.e., Ag/PATP/Au) no enhancement of the b_2 modes was observed.

In this work we explore the results of fabrication of a sandwich structure between a metal (Ag) and a semiconductor (ZnO) mediated by PATP. The band gap of ZnO is rather large (3.35 eV) so that net charge transfer can only be achieved from the metal to the semiconductor. We consider two systems: the first involves depositing a layer of PATP on a ZnO film and then adding Ag nanoparticles. This system (ZnO/PATP/Ag) has the thiol attached to the ZnO and the amino group attached to the Ag nanoparticle. In the second system the order is reversed (Ag/PATP/ZnO), and the thiol is attached to the Ag, with the amino end attached to the ZnO. In the former assembly we find that the b_2 modes of PATP are strongly enhanced in the SERS spectrum, whereas in the latter, they are not. The appearance of nontotally symmetric (b_2) modes is diagnostic of a charge-transfer process. This indicates that charge is transferred in the ZnO/PATP/Ag system but not in the reverse system. We examine the likely mechanism of charge transfer in this system.

II. Experimental Procedures

Chemicals. All the reagents were used as received without further purification. Silver nitrate was obtained from Aldrich. 4-Aminothiophenol (PATP) was obtained from Acros Organics Chemical Co. Poly(diallydimethylammonium chloride) (PDDA) with medium molecular weight (200 000−350 000) was obtained from Sigma Chemical Company. Zinc nitrate was obtained from the Beijing Chem. Co. (China). Ethanol was purchased from Beijing Chem. Co. (China).

Apparatus and Methods. *Synthesis of Silver Colloid.* Silver colloid was prepared according to the literature protocols.[27] The particular description is as follows: $AgNO_3$, (36 mg) was dissolved in 200 mL of H_2O and brought to a boil. A solution of 1% sodium citrate (4 mL) was added. The solution was kept boiling for about 1 h. The Ag colloid was greenish yellow and displayed an absorption maximum at 410 nm.

Preparation of ZnO Nanorod Films. ZnO nanorod films were prepared according to literature protocols.[28] Glass slides were suspended in an aqueous solution of zinc nitrate hydrate, $Zn(NO_3)_2 \cdot H_2O$, (0.025 M) and methenamine (0.025 M) at 90 °C for 3 h. ZnO nanorods were grown directly on the glass substrates, and they were removed from the solution, rinsed with deionized water, dried, and stored in the dark under clean air.

Preparation of ZnO/ATP/Ag Sandwich Structure (Figure 1*a*). Self-assembled monolayers were deposited by immersing freshly prepared ZnO nanorod film substrates into 0.1 mM PATP solution in ethanol at room temperature for 24 h. After deposition, the sample was taken out from the reactor and rinsed three times with ethanol and deionized water, respectively. Then the prepared ZnO/ATP film was immersed in silver colloid for 30 min, the sample was taken out from the reactor, rinsed three times with deionized water, and dried under N_2 stream.

Preparation of Ag/ATP/ZnO Sandwich Structure (Figure 1b). The glass slides were cleaned by immersion in a boiling solution prepared by mixing 30% H_2O_2 and concentrated H_2SO_4 with a volume ratio of 3:7. After cooling, the substrates were rinsed repeatedly with deionized water. The slides were then immersed in a 0.5% PDDA solution for about 40 min and finally rinsed with triply deionized water. The slides were immersed into the silver colloid for about 3 h. The slides were then rinsed with deionized water and immersed in 0.1 mM PATP solution for 30 min and rinsed with ethanol and deionized water, respectively. Finally, a film of ZnO nanorods was deposited on the prepared Ag/ATP substrate through the method mentioned above.

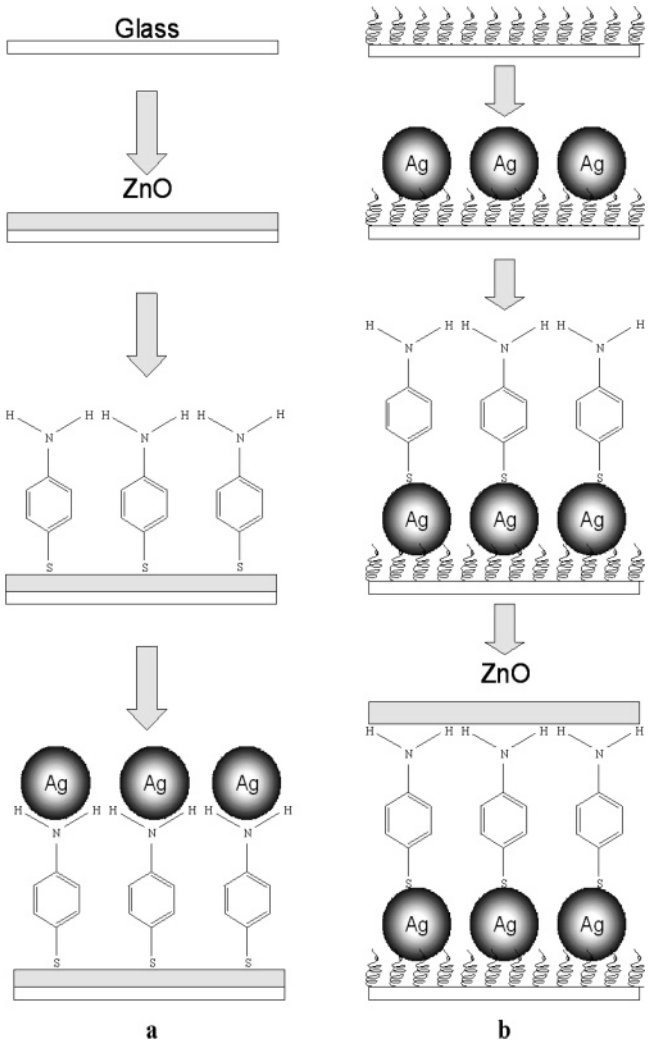

Figure 1. Schematic illustration of the structure of ZnO/PATP/Ag (a) and Ag/PATP/ZnO (b) molecular junctions on glass substrates.

The extinction spectra were measured on a Shimadzu UV-3600 spectrometer. The surface morphologies of the samples were measured on a JEOL JSM-6700F field emission scanning electron microscope (FE-SEM) operating at 3.0 keV. Surface-enhanced Raman spectra were measured on a Nicolet 960 FT-Raman spectrometer equipped with a liquid-nitrogen-cooled Ge detector and a Nd:VO_4 laser (1064 nm) as excitation source (the laser power used was about 250 mW at the samples) and a Renishaw Raman system model 1000 spectrometer with the 514.5 nm argon ion laser exciting source (the laser power at the sample position was typically 400 μW with an average spot size of 1 μm in diameter). The spectral resolution was 4 cm^{-1} at the excitation wavelength.

III. Results

In Figure 2 we show the SEM images of (Figure 2a) ZnO crystal film and (Figure 2b) ZnO/PATP/Ag assemblies. The ZnO film is seen to be composed of a collection of hexagonal nanorods approximately 0.5−2 μm in diameter. They are little changed by absorption of PATP, whereas the Ag colloid particles can clearly be seen in the image Figure 2b.

In Figure 3 we present the extinction spectra of (Figure 3a) the ZnO film, (Figure 3b) the ZnO/PATP assembly, (Figure 3c) the ZnO/PATP/Ag assembly, (Figure 3d) a Ag colloid, and

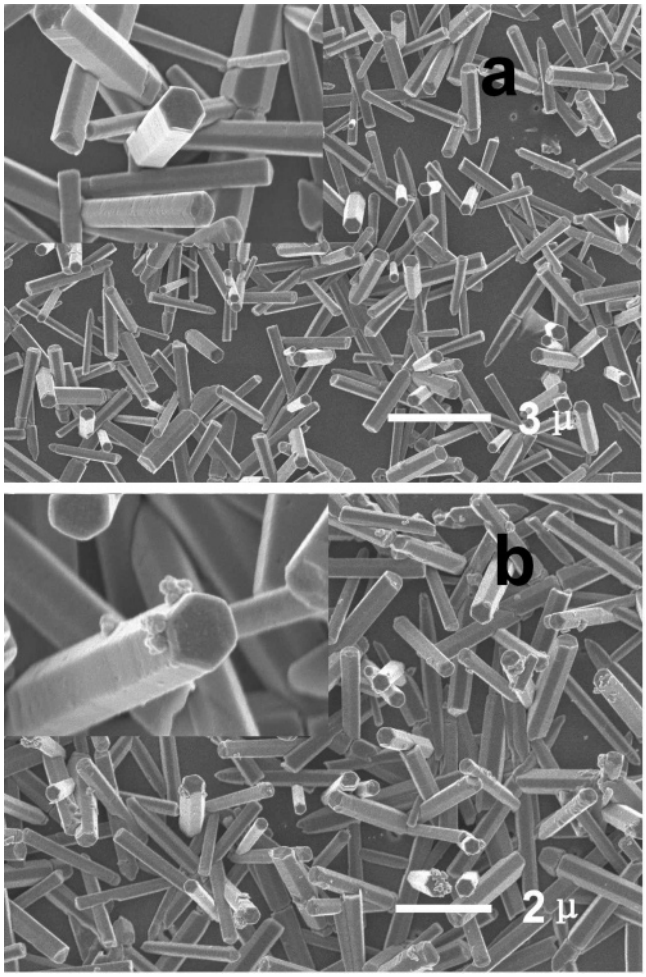

Figure 2. SEM images of (a) ZnO crystal film and (b) ZnO/PATP/Ag assemblies.

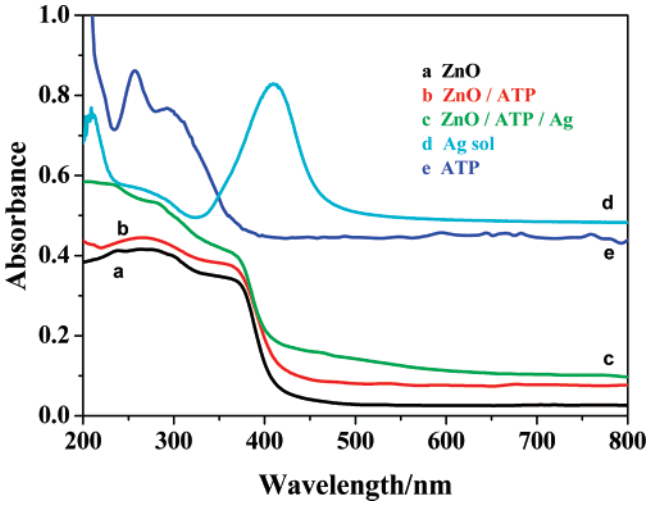

Figure 3. Extinction spectra of (a) ZnO film, (b) the ZnO/PATP assembly, (c) the ZnO/PATP/Ag assembly, (d) a Ag colloid, and (e) PATP molecules in ethanol solutions.

(Figure 3e) PATP molecules in ethanol solutions. The ZnO film shows a broad band below 400 nm, while addition of the PATP introduces a UV peak near 290 nm (similar to a broadened solution spectrum of PATP shown in Figure 3e). Addition of the Ag nanoparticles causes the two PATP bands to shift to around 300 nm. For comparison, we show the Ag colloid

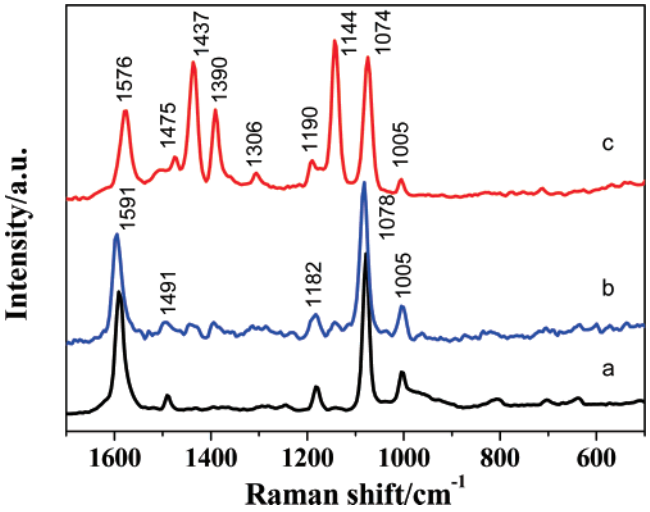

Figure 4. Raman spectra (at 1064 nm) of the PATP molecules (a) adsorbed on the silver nanoparticle monolayer, (b) in the Ag/PATP ZnO assembly, and (c) the ZnO/PATP/Ag assembly.

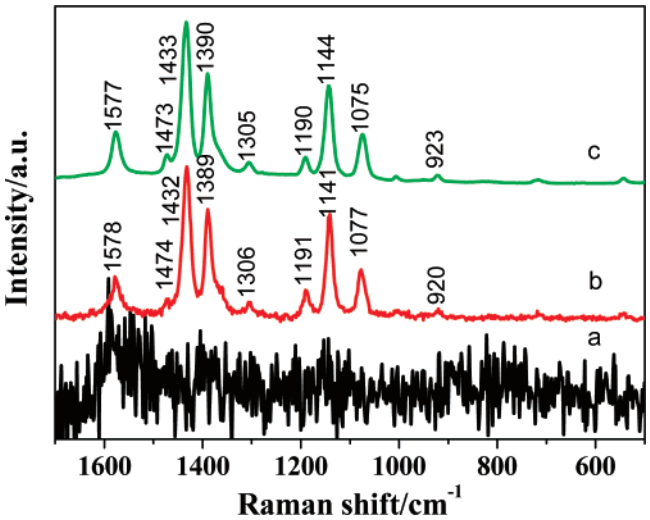

Figure 5. Raman spectra excited at 514.5 nm of the PATP molecules (a) adsorbed on the surface of a ZnO nanoparticle, (b) adsorbed on the silver surface, and (c) the ZnO/PATP/Ag assembly.

spectrum, in which a characteristic single broad band centered at around 400 nm is seen. There is little hint of this band in the ZnO/PATP/Ag assembly spectrum, probably due to the relatively low concentration of Ag particles in the assembly, as shown in Figure 2.

In Figure 4, we show the Raman spectra excited at 1064 nm of the PATP molecules (Figure 4a) adsorbed on the surface of Ag nanoparticle layer, (Figure 4b) Ag/PATP/ZnO assembly, and (Figure 4c) on the ZnO/PATP/Ag assembly. Note that on the Ag surface or the Ag/PATP/ZnO, PATP shows only two intense bands at 1089 and 1591 cm^{-1} at this exciting wavelength. These spectra are consistent with other spectra of this molecule under the same circumstances. However, on the ZnO/PATP/Ag assembly, several other intense lines, namely, at 1144, 1306, 1390, and 1437 cm^{-1}, are observed as strongly enhanced. Furthermore there are shifts of the two lines originally observed to lower wavenumbers. We will discuss the interpretation of these results in the next section.

In Figure 5, we show the results of Raman spectra of excited at 514.5 nm of the PATP molecules (Figure 5a) adsorbed on

TABLE 1: Raman Frequencies and Assignments of 4-Aminothiophenol (PATP) in the 800−1800 cm^{-1} Region[a]

	Ag film		ZnO/PATP/Ag			
solid 1064 nm[b]	1064 nm	514.5 nm	1064 nm	514.5 nm	assignment	mode/sym.
1595s	1591s				C═C str	8a/a_1
1572[c]		1578m	1576m	1577m	C═C str	8b/b_2
1490w	1491w	1474w	1475w	1473w	C═C str + CH ip bend	19a/a_1
1445vw	1442vw	1432s	1437s	1433s	C═C str + CH ip bend	19b/b_2
1403w	1392vw	1389s	1390m	1390s	CH ip bend + C═C str	3/b_2
1310vw		1306w	1306w	1305w	C═C str + CH ip bend	14/b_2
1173m	1182w	1191w	1190m	1190w	CH ip bend	9a/a_1
1142vw	1144vw	1141s	1144s	1044s	CH ip bend	9b/b_2
1089s	1078s	1077m	1074s	1075m	CS str	7a/a_1
1011w	1005w	1005w	1005w	1005w	CC ring def	18a/a_1

[a] Intensities: s = strong, m = medium, w = weak. [b] Frequencies (in cm^{-1}) followed by relative intensities (s, strong; m, medium; w, weak, vw, very weak). [c] Bands observed only in the UVRR spectrum at 309.1 nm excitation (ref 30).

the surface of ZnO nanoparticle, (Figure 5b) adsorbed on the silver surface, and (Figure 5c) ZnO/PATP/Ag assembly. Note that on the ZnO surface alone, there is almost no Raman intensity, whereas on the Ag surface and the ZnO/PATP/Ag assembly a spectrum similar to that of Figure 4c is obtained. This shows that the observed spectrum is not due to the ZnO substrate alone but does appear when the molecule is attached to a SERS-active Ag colloid. In the latter case the adsorption is known to be through the thiol end of the molecule, and the charge-transfer effect is evident at this exciting wavelength.

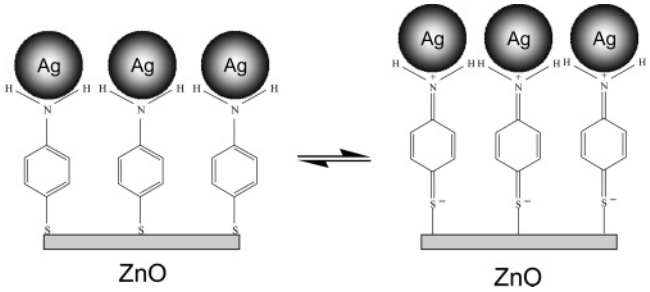

Figure 6. Resonance structures of the ZnO/ATP/Ag assembly.

IV. Discussion

The results presented in the previous section show that there is a sharp difference in the observed Raman spectrum between the ZnO/PATP/Ag assembly and the Ag/PATP/ZnO assembly. In Table 1 we present a summary of the observed wavenumbers and assignments of the modes observed in the various spectra. The assignments were taken from ref 25 and confirmed with our own DFT calculation, using the Gaussian 03 suite of programs on a SGI-3900 computer system by B3LYP with the 6-31++G(d,p) basis set. The vibrational characteristics of para-disubstituted benzenes are given by notations of the corresponding vibrations of benzene[29] together with the symmetry species under an assumption of C_{2v} symmetry. The benzene ring vibrations are classified as a_1, a_2, b_1, and b_2 species. The a_1 and b_2 species are in-plane modes, and a_2 and b_1 species are out-of-plane modes.

For the normal Raman spectra of PATP molecules, the predominant peaks located at 1595 and 1089 cm^{-1} were assigned to the a_1 modes of the PATP molecules. Some other weak bands at 1572, 1445, 1403, and 1142 cm^{-1} were assigned to the b_2 modes.

Notice in the ZnO/PATP/Ag assembly (see also Figure 4c) that the lines at 1144, 1306, 1390, and 1437 cm^{-1} are strongly enhanced. These are all of b_2 symmetry, and their strong enhancement is taken to be evidence of charge transfer. The charge-transfer mechanism in SERS is a result of Herzberg−Teller (vibronic) coupling between various molecular and metal states.[13] The mechanism is intensity borrowing from an allowed molecular transition, but strict selection rules apply. Since the molecule is perpendicular to the Ag surface the charge-transfer transition moment must by of A_1 symmetry (in C_{2v}) with respect to the molecular orientation. The most intense transition available for borrowing is the $\pi \rightarrow \pi^*$ transition at 300 nm, which is of B_2 symmetry.[30] Thus the Herzberg−Teller selection rule tells us that the $A_1 \times B_2 = b_2$ vibrational modes should be enhanced, exactly as observed.

In Figure 6, we illustrate the fact that for the ZnO/PATP/Ag assembly there is a strong propensity for the dipolar quinoid-like resonance structure $NH_2^+{=}\phi{=}S^-$ to be an important contributor to the stability of the assembly. The electronegative $=S^-$ atom is attached to a Zn^{2+} site on the semiconductor, whereas the $=NH_2^+$ end of the molecule is attached to the Ag nanoparticle. With charge transfer from the conduction band of the Ag nanoparticle to the π^* level (LUMO) of the molecule, the added electron weakens the resonance structure, lowering the bond order, resulting in downshifts in the vibrations sensitive to this resonance structure. These are, namely, the 1595 and the 1089 cm^{-1} lines, which shift to 1576 and 1074 cm^{-1}, respectively. The 1595 cm^{-1} line is the C═C stretch, and the 1089 cm^{-1} line is the C−S stretch. The frequency shifts are due to the strong interaction between adsorbate and substrate. The difference of substrate also caused little difference in the Raman shift.

In Figure 7, we illustrate the difference between the two assemblies. Note that for the ZnO/PATP/Ag assembly the Ag nanoparticles can readily donate electrons to the relatively electropositive $=NH_2^+$ part of the molecule, while the $=S^-$ end can readily donate an electron to the ZnO. Thus, the direction of charge transfer, from Ag to ZnO, is facile. However, in the Ag/PATP/ZnO structure, the relatively negative $=S^-$ resists electron transfer from the Ag nanoparticles, and the same is true for the $=NH_2^+$/ZnO interface.

These ideas are made more concrete by the energy level diagram in Figure 8. The Fermi level for Ag is 4.3 eV below the vacuum level, while the ionization potential of PATP is 7.16 eV.[31] This is the location of the lowest filled orbital (HOMO). The lowest unfilled orbital (LUMO) should correspond to the 300 nm transition, putting it at 3.03 eV. The valence band of ZnO is at 7.7 eV below the vacuum level, and the band gap is 3.35 eV, locating the bottom of the conduction band at 4.3 eV. The Fermi level of ZnO is just slightly below this. It can readily be seen from this diagram, that the introduction of a photon at

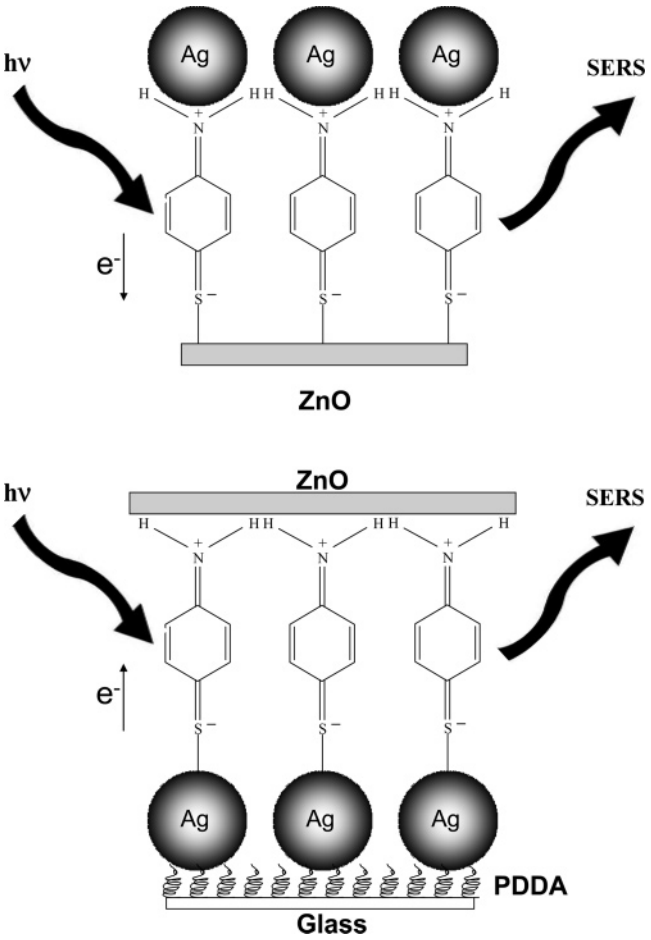

Figure 7. Charge-transfer mode of ZnO/PATP/Ag and Ag/PATP/ZnO assemblies under light.

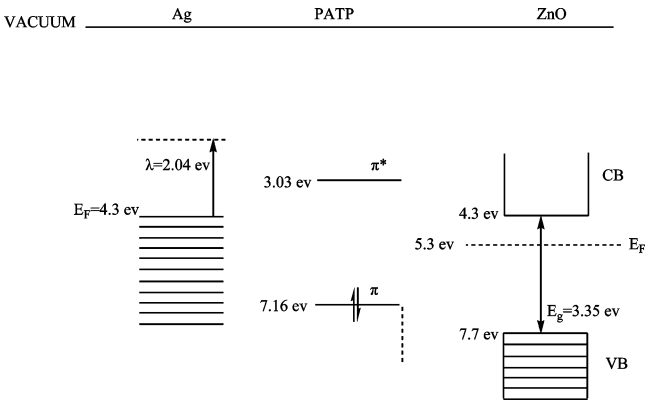

Figure 8. Energy level diagram of the ZnO/PATP/Ag assembly. All levels are measured from the vacuum.

514.5 nm (2.40 eV) will be sufficient to easily transfer an electron to an excited unfilled level of PATP, which can then easily transfer it to the conduction band of ZnO. As the ZnO conduction band is filled, the ZnO Fermi level rises, while the Ag Fermi level falls. Equilibrium is reached when both Fermi levels (or chemical potentials) are the same. At this point the rate of charge transfer in both directions is equal, stabilizing the SERS signal. A similar Fermi level equilibration has been observed between TiO_2 and single-wall carbon nanotubes.[32] A glance at the energy level diagram will also show that the reverse process (i.e., starting with charge transfer from the ZnO to the Ag particles) is not energetically possible. The highest filled electron level in ZnO is 7.7 eV below the vacuum, and there is not enough energy in the incoming photon to initiate a charge-transfer process in this direction.

The system examined here can be regarded as part of a class of assemblies, which behave as molecular rectifiers. In a recent electrochemical study of nonequilibrium electronic charge transport in 4,4′-bipyridine sandwiched between two Au(111) surfaces, Wu et al.[33] showed that when the Fermi level of the metal lies close to an unoccupied π^* molecular orbital energy, electronic charge transfer is facilitated. Kim and Yoon[34] examined PATP sandwiched between Ag or Au nanoparticles and a smooth Au surface. Using SERS they examined the relative contribution of plasmonic coupling and charge transfer to the Raman signal. A more complete discussion of molecular rectifiers is provided in a review by Metzger,[35] concentrating on single-molecule effects.

Acknowledgment. This research was supported by the NSFC (Grant Nos. 20473029, 20573041, 20773044) of the People's Republic of China, the Program for Changjiang Scholars and Innovative Research Team in University (IRT0422), the Program for New Century Excellent Talents in University, and the 111 Project (B06009). We are also indebted to the National Institute of Justice (Department of Justice Award No. 2006-DN-BX-K034) and the City University Collaborative Incentive Program (No. 80209). This work was also supported by the National Science Foundation under Cooperative Agreement No. RII-9353488, Grant Nos. CHE-0091362, CHE-0345987 and Grant No. ECS0217646 and by the City University of New York PSC-BHE Faculty Research Award Program.

References and Notes

(1) Van Duyne, R. P. In "*Chemical and Biochemical Applications of Lasers*"; Moore, C. B., Ed.; Academic Press: New York, 1979; Vol. 4, Chapter 5.
(2) Nie, S. M.; Emory, S. R. *Science* **1997**, *275*, 1102−1106.
(3) Kneipp, K.; Wang, Y.; Kneipp, H.; Perelman, L. T.; Itzkan, I.; Dasari, R. R.; Feld, M. S. *Phys. Rev. Lett.* **1997**, *78*, 1667−1670.
(4) Tian, Z. Q.; Ren, B. *Annu. Rev. Phys. Chem.* **2004**, *55*, 197−229.
(5) Lee, S. J.; Morrill, A. R.; Moskovits, M. *J. Am. Chem. Soc.* **2006**, *128*, 2200−2201.
(6) Tian, Z. Q.; Ren, B.; Wu, D. Y. *J. Phys. Chem. B* **2002**, *106*, 9463−9483.
(7) Moskovits, M. *Rev. Mod. Phys.* **1985**, *57*, 783−826.
(8) Haynes, C. L.; McFarland, A. D.; Van Duyne, R. P. *Anal. Chem.* **2005**, *77*, 338A−346A.
(9) Xu, H. X.; Aizpurua, J.; Kall, M.; Apell, P. *Phys. Rev. E* **2000**, *62*, 4318−4324.
(10) Stockman, M. I. *Top. Appl. Phys.* **2006**, *103*, 47−66.
(11) Brown, R. J. C.; Wang, J.; Tantra, R.; Yardley, R. E.; Milton, M. J. T. *Faraday Disscuss.* **2006**, *132*, 201−213.
(12) Otto, A. *J. Raman Spectrosc.* **2005**, *36*, 497−509.
(13) Lombardi, J. R.; Birke, R. L.; Lu, T. H.; Xu, J. *J. Chem. Phys.* **1986**, *84*, 4174−4180.
(14) Lombardi, J. R.; Birke, R. L.; Sanchez, L. A.; Bernard, I.; Sun, S. C. *Chem. Phys. Lett.* **1984**, *104*, 240−247.
(15) Quagliano, L. G. *J. Am. Chem. Soc.* **2004**, *126*, 7393−7398.
(16) Wang, Y. F.; Sun, Z. H.; Wang, Y. X.; Hu, H. L.; Zhao, B.; Xu, W. Q.; Lombardi, J. R. *Spectrochim. Acta, Part A* **2007**, *66*, 1199−1203.
(17) Wang, Y. F.; Sun, Z. H.; Hu, H. L.; Jing, S. Y.; Zhao, B.; Xu, W. Q.; Zhao, C.; Lombardi, J. R. *J. Raman Spectrosc.* **2007**, *38*, 34−38.
(18) Wang, Y. F.; Hu, H. L.; Jing, S. Y.; Wang, Y. X.; Sun, Z. H.; Zhao, B.; Zhao, C.; Lombardi, J. R. *Anal. Sci.* **2007**, *23*, 787−791.
(19) Sun, Z. H.; Zhao, B.; Lombardi, J. R. *Appl. Phys. Lett.* **2007**, *91*, 221106.
(20) Louie, S. G.; Chelikowsky, J. R.; Cohen, M. L. *Phys. Rev. B* **1977**, *15*, 2154−2162.
(21) Tejedor, C.; Flores, F.; Louis, E. *J. Phys. C: Solid State Phys.* **1977**, *10*, 2163−2177.
(22) Shan, G. Y.; Xu, L. H.; Wang, G. R.; Liu, Y. C. *J. Phys. Chem. C* **2007**, *111*, 3290−3293.
(23) Zhou, Q.; Zhao, G.; Chao, Y. W.; Li, Y.; Wu, Y.; Zheng, J. W. *J. Phys. Chem. C* **2007**, *111*, 1951−1954.

(24) Maniu, D.; Chis, V.; Baia, M.; Toderas, F.; Astelan, S. *J. Optoelectron. Adv. Mater.* **2007**, *9*, 733−736.
(25) Zhou, Q.; Li, X. W.; Fan, Q.; Zhang, X. X.; Zheng, J. W. *Angew. Chem., Int. Ed.* **2006**, *45*, 3970−3973.
(26) Zhou, Q.; Chao, Y. W.; Li, Y.; Xu, W.; Wu, Y.; Zheng, J. W. *ChemPhysChem* **2007**, *8*, 921−925.
(27) Lee, P. C.; Meisel, D. *J. Phys. Chem.* **1982**, *86*, 3391−3395.
(28) Feng, X. J.; Feng, L.; Jin, M. H.; Zhai, J.; Jiang, L.; Zhu. D. B. *J. Am. Chem. Soc.* **2004**, *126*, 62−63.
(29) Wilson, E. B., Jr. *Phys. Rev.* **1934**, *45*, 706.
(30) Osawa, M.; Matsuda, N.; Yoshii, K.; Uchida, I. *J. Phys. Chem.* **1994**, *98*, 12702−12707.
(31) Larsen, A. G.; Holm, A.; Roberson, M.; Daasbjerg, K. *J. Am. Chem. Soc.* **2001**, *123*, 1723−1729.
(32) Kongkanand, A.; Kamat, P. V. *ACS Nano* **2007**, *1*, 13.
(33) Wu, X.; Li, Q.; Huang, J.; Yang, J. *J. Chem. Phys.* **2005**, *123*, 184712.
(34) Kim, K.; Yoon, J. K. *J. Phys. Chem. B* **2005**, *109*, 20731−20736.
(35) Metzger, R. M. *Chem. Rev.* **2003**, *103*, 3803−3834.